*Chemistry Research Journal*, 2017, 2(4):198-213

*Available online www.chemrj.org*

**Research Article**

**ISSN: 2455-8990**
**CODEN(USA): CRJHA5**

# A Theoretical Study of the Relationships between Electronic Structure and 5-$HT_{1A}$ and 5-$HT_{2A}$ Receptor Binding Affinity of a group of ligands containing an isonicotinic nucleus

**Juan S. Gómez-Jeria*, Jorge Abuter-Márquez**

Quantum Pharmacology Unit, Department of Chemistry, Faculty of Sciences, University of Chile. Las Palmeras 3425, Santiago 7800003, Chile

**Abstract** A formal quantum-chemical analysis of the relationships between the electronic structure of two series of isonicotinamide derivatives and their 5-$HT_{1A}$ and 5-$HT_{1B}$ receptor binding affinities was carried out. The electronic structure was calculated at the B3LYP/6-31G(d,p) after full geometry optimization. Statistically significant relationships were obtained for the four cases. The analysis of the results suggests what modifications of the molecules could be useful to raise receptor affinity. The partial 2D pharmacophores for the binding to each receptor suggest that both, 5-$HT_{1A}$ and 5-$HT_{2A}$, seem to have a site that is rich in sigma electrons.

**Keywords** Serotonin, QSAR, KPG method, 5-$HT_{1A}$, 5-$HT_{2A}$, pharmacophore, reactivity indices

## Introduction

Serotonin receptors are a group of G protein-coupled receptors and ligand-gated ion channels found in the central and peripheral nervous systems. As their subtypes and effects have been discussed in previous publications, we refer the reader to the literature [1, 2]. Some of the main latest advances that deserve to be mentioned are in Refs. [3-9].

From a longtime our Unit has been studying the relationships between electronic structure and serotonergic receptor(s) binding affinity in structurally different groups of molecules [1, 2, 10-20]. As a new effort to get more information about these systems, we present here the results of quantum chemical study of the relationships between 5-$HT_{1A}$ and 5-$HT_{2A}$ receptor binding affinity and the electronic structure of a series of isonicotinamide derivatives.

## Methods, models and calculations

The molecules were selected from a recent study[21]. They are shown in Figs. 1 and 2, and Tables 1 and 2[21]. The biological activity studied here is the in vitro affinity for serotonin $5HT_{1A}$ and $5HT_{2A}$ receptors measured in rat brain cortex with radioligand binding assays ([$^3$H]8-OH-DPAT for $5HT_{1A}$ receptors and [$^3$H] ketanserin for $5HT_{2A}$ receptors), expressed as $IC_{50}$[21].

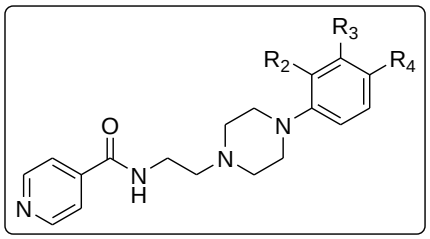


*Figure 1: General structure of molecules of Group A*

**Table 1**: Structure and receptor affinities of Group A [21].

| Mol. | Mol. | $R_2$ | $R_3$ | $R_4$ | $\log(IC_{50})$ $5HT_{1A}$ | $\log(IC_{50})$ $5HT_{2A}$ |
|---|---|---|---|---|---|---|
| 1 | 3a | H | H | H | 0.94 | 2.30 |
| 2 | 3b | OMe | H | H | -0.44 | 2.77 |
| 3 | 3c | H | H | OMe | 3.10 | 2.96 |
| 4 | 3d | $OCH_2CH_3$ | H | H | 0.68 | 1.21 |
| 5 | 3e | CN | H | H | 1.18 | 1.74 |
| 6 | 3f | $CH_3$ | H | H | 2.74 | 2.80 |
| 7 | 3g | $CH_3$ | $CH_3$ | H | 1.22 | 1.85 |
| 8 | 3h | Cl | H | H | 0.45 | 2.67 |
| 9 | 3i | H | Cl | H | -0.09 | 1.55 |
| 10 | 3j | H | H | Cl | 2.52 | 2.82 |
| 11 | 3k | H | Cl | Cl | 2.66 | 0.99 |
| 12 | 3l | F | H | H | 1.03 | -1.90 |
| 13 | 3m | H | H | F | 2.74 | -1.34 |
| 14 | 3n | H | H | H | 0.03 | - |
| 15 | 3o | -* | H | H | 2.20 | 3.44 |
| 16 | 3t | H | H | H | 0.72 | 1.62 |

*:N instead of C.

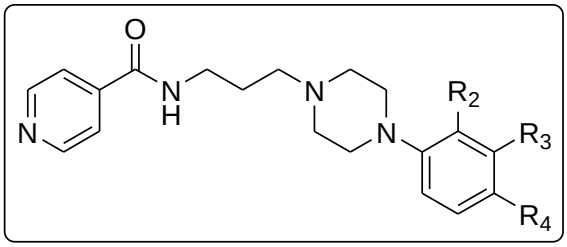


*Figure 2: General structure of molecules of Group B*

**Table 2**: Structure and receptor affinities of Group B [21].

| Mol. | $R_2$ | $R_3$ | $R_4$ | $\log(IC_{50})$ $5HT_{1A}$ | $\log(IC_{50})$ $5HT_{2A}$ |
|---|---|---|---|---|---|
| 1 | H | H | H | 1.75 | 2.05 |
| 2 | OMe | H | H | 1.14 | -0.60 |
| 3 | H | H | OMe | 1.39 | 3.10 |
| 4 | $OCH_2CH_3$ | H | H | 0.98 | 2.32 |
| 5 | CN | H | H | 2.09 | 2.26 |
| 6 | $CH_3$ | H | H | 3.52 | - |
| 7 | $CH_3$ | $CH_3$ | H | 0.93 | 2.89 |
| 8 | Cl | H | H | 2.09 | 1.97 |
| 9 | H | Cl | H | 2.77 | 3.14 |
| 10 | H | H | Cl | 2.51 | 0.55 |
| 11 | H | Cl | Cl | 2.34 | 0.03 |
| 12 | F | H | H | 2.52 | -1.41 |
| 13 | H | H | F | 2.00 | -0.64 |
| 14 | H | H | H | 2.00 | 2.90 |
| 15 | -* | H | H | 0.96 | -2.01 |
| 16 | H | H | H | 3.03 | - |

*:N instead of C.

To relate structure with activity we employed the formal KGP (Klopman-Peradejordi-Gómez) method [22]. As this technique has been the subject of a recent full review we refer the reader to the literature [23-30]. In summary, any

biological activity is related through a linear equation to a set of local atomic reactivity indices and the orientational parameters of the substituents. The applications of the KPG method to diverse biological activities and molecule during 2016-2017 showed its superiority over the empirical QSAR methods [2, 31-45].

The electronic structure of all molecules in their protonated form was calculated with the Density Functional Theory at the B3LYP/6-31G(d,p) level after full geometry optimization. The Gaussian suite of programs was used [46]. The numerical values for the LARIs were calculated from information inside the Gaussian results file with the D-Cent-QSAR software [47]. All the electron populations smaller than or equal to 0.01 e were considered as zero[24]. Negative electron populations coming from Mulliken Population Analysis were corrected as usual[48]. Orientational parameters were taken from published Tables or calculated as usual [49-51]. Given that the resolution of the system of linear equations is not possible because we have not enough experimental data, we employed Linear Multiple Regression Analysis (LMRA) techniques to find the best solution. For each case, a matrix containing the dependent variable ($\log(IC_{50})$) and the local atomic reactivity indices of all atoms of the common skeleton as independent variables was built. The Statistica software was used for LMRA [52].

**Results**

Results for Group A

Figure 3 shows the common skeleton numbering of Group A that will be employed in the results and discussion.

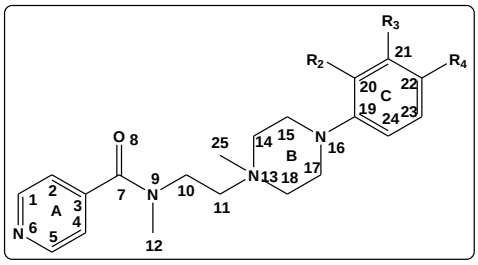


*Figure 3: Common skeleton numbering for Group A*

Results for the 5-$HT_{1A}$receptor binding affinity of Group A.

The best equation obtained is:

$$\log(IC_{50}) = 37.37 + 0.02\phi_4 + 0.50S_{19}^{E} - 30.5S_{12}^{E}(HOMO-2)^{*} - 168.20F_4(LUMO)^{*} \quad (1)$$

with n=13, R=0.98, $R^2$=0.96, adj-$R^2$=0.94, F(4,8)=49.23($p<0.00001$) and a standard error of estimate of0.23. No outliers were detected and no residuals fall outside the $\pm 2\sigma$ limits. Here, $\varphi_4$ is the orientational parameter of $R_4$, $S_{19}^{E}$ is the total atomic electrophilic superdelocalizability of atom 19, $S_{12}^{E}$(HOMO-2)* is the electrophilic superdelocalizability of the third highest occupied molecular orbital localized on atom 12 and $F_4$(LUMO)* is the Fukui index (electron population) of the lowest empty MO localized on atom 4. Tables 3 and 4 show the beta coefficients, the results of the t-test for significance of coefficients and the matrix of squared correlation coefficients for the variables of Eq. 1. There are no significant internal correlations between independent variables (Table 4). Figure 4 displays the plot of observed *vs.* calculated $\log(IC_{50})$.

**Table 3**: Beta coefficients and t-test for significance of coefficients in Eq. 1

| Variable | Beta | t(8) | p-level |
|---|---|---|---|
| $\varphi_4$ | 0.64 | 8.86 | 0.00002 |
| $S_{19}^{E}$ | 0.22 | 2.94 | 0.019 |
| $S_{12}^{E}$(HOMO-2)* | -0.47 | -6.30 | 0.0002 |
| $F_4$(LUMO)* | -0.29 | -3.56 | 0.0074 |

**Table 4**: Matrix of squared correlation coefficients for the variables in Eq. 1

| | $\varphi_4$ | $S_{19}^E$ | $S_{12}^E$(HOMO-2)* | $F_4$(LUMO)* |
|---|---|---|---|---|
| $\varphi_4$ | 1.00 | | | |
| $S_{19}^E$ | 0.00 | 1.00 | | |
| $S_{12}^E$(HOMO-2)* | 0.00 | 0.01 | 1.00 | |
| $F_4$(LUMO)* | 0.06 | 0.11 | 0.07 | 1.00 |

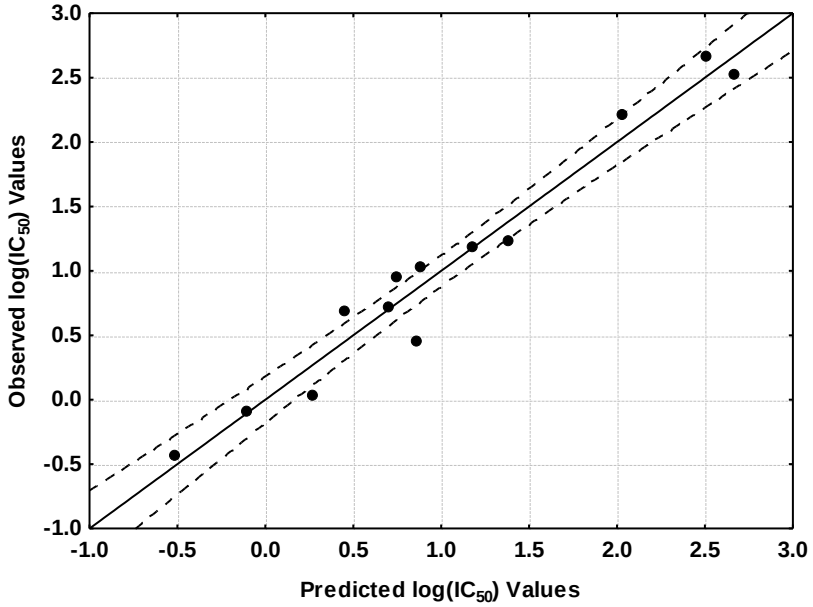


*Figure 4: Plot of predicted vs. observed log($IC_{50}$) values (Eq. 1). Dashed lines denote the 95% confidence interval*

The associated statistical parameters of Eq. 1 indicate that this equation is statistically significant and that the variation of the numerical values of a group of four local atomic reactivity indices of atoms of the common skeleton explains about 94% of the variation of log($IC_{50}$). Figure 4, spanning about 3.5 orders of magnitude, shows that there is a good correlation of observed *versus* calculated values and that almost all points are inside the 95% confidence interval.

Results for the 5-$HT_{2A}$receptor binding affinity of Group A

The best equation obtained is:

$$\log(IC_{50}) = -17.44 - 11.99S_8^E(HOMO-1)^* - 72.14F_{15}(HOMO-2)^* - 2.06\mu_{10} + \\ +0.24S_{23}^N(LUMO+2)^* + 1.52F_{21}(HOMO-1)^* \quad (2)$$

with n=14, R=0.99, $R^2$=0.99, adj-$R^2$=0.98, F(5,8)=147.63 ($p<0.000001$) and a standard error of estimate of0.20. No outliers were detected and no residuals fall outside the $\pm 2\sigma$ limits. Here, $S_8^E$(HOMO-1)* is the electrophilic superdelocalizability of the second highest occupied MO localized on atom 8, $F_{15}$(HOMO-2)* is the Fukui index of the third occupied MO localized on atom 15, $\mu_{10}$ is the local atomic electronic chemical potential of atom 10, $S_{23}^N$(LUMO+2)* is the nucleophilic superdelocalizability of the third empty MO localized on atom 23 and $F_{21}$(HOMO-1)* is the Fukui index of the second highest occupied MO localized on atom 21.Tables 5 and 6 show the beta coefficients, the results of the t-test for significance of coefficients and the matrix of squared correlation coefficients for the variables of Eq. 2. There are no significant internal correlations between independent variables (Table 6). Figure 5 displays the plot of observed *vs.* calculated log($IC_{50}$).

**Table 5**: Beta coefficients and t-test for significance of coefficients in Eq. 2

| Variable | Beta | t(8) | p-level |
|---|---|---|---|
| $S_8^E$(HOMO-1)* | -0.82 | -20.81 | 0.0000001 |
| $F_{15}$(HOMO-2)* | -0.70 | -16.93 | 0.0000001 |
| $\mu_{10}$ | -0.26 | -6.57 | 0.0002 |
| $S_{23}^N$(LUMO+2)* | 0.30 | 6.68 | 0.0002 |
| $F_{21}$(HOMO-1)* | 0.17 | 3.73 | 0.006 |

**Table 6**: Matrix of squared correlation coefficients for the variables in Eq. 2

| | $S_8^E$(HOMO-1)* | $\mu_{10}$ | $F_{15}$(HOMO-2)* | $F_{21}$(HOMO-1)* |
|---|---|---|---|---|
| $\mu_{10}$ | 0.02 | 1.00 | | |
| $F_{15}$(HOMO-2)* | 0.01 | 0.07 | 1.00 | |
| $F_{21}$(HOMO-1)* | 0.05 | 0.03 | 0.09 | 1.00 |
| $S_{23}^N$(LUMO+2)* | 0.07 | 0.05 | 0.04 | 0.14 |

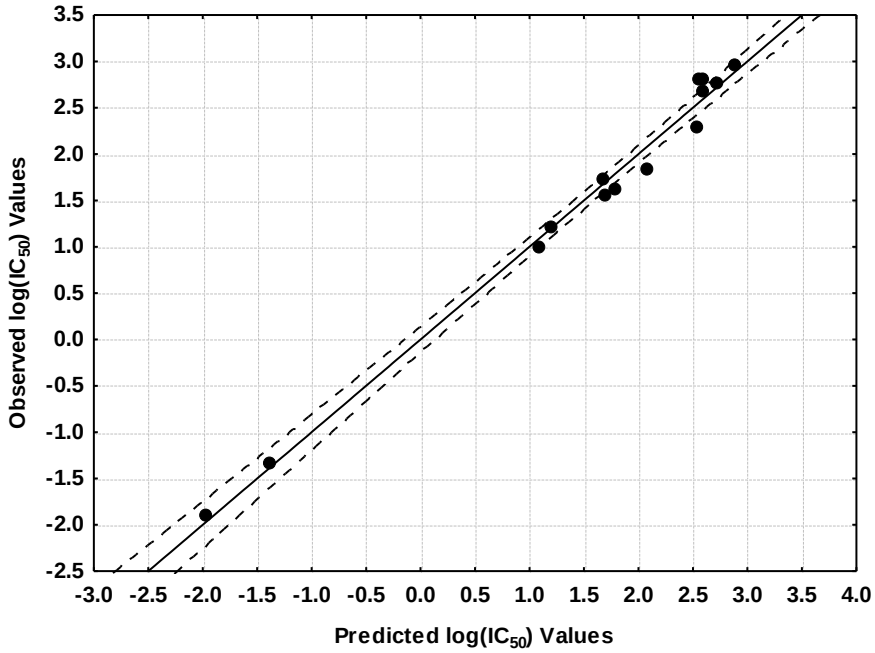


*Figure 5: Plot of predicted vs. observed log($IC_{50}$) values (Eq. 2). Dashed lines denote the 95% confidence interval*

The associated statistical parameters of Eq. 2 indicate that this equation is statistically significant and that the variation of the numerical values of a group of five local atomic reactivity indices of atoms of the common skeleton explains about 98% of the variation of the receptor affinity. Figure 5, spanning about five orders of magnitude, shows that there is a good correlation of observed *versus* calculated values and that almost all points are inside the 95% confidence interval.

Local Molecular Orbitals

Table 7 shows the local molecular orbitals of atoms 4, 8 and 12. Table 8 shows the local molecular orbitals of atoms 15, 21 and 23 (see Fig. 3). Nomenclature: Molecule (HOMO) / (HOMO-2)* (HOMO-1)* (HOMO)* - (LUMO)* (LUMO+1)* (LUMO+2)*.

**Table 7**: Local Molecular Orbitals of atoms 4, 8 and 12

| Molecule | Atom 4 (C) | Atom 8 (O) | Atom 12 (H) |
|---|---|---|---|
| 1 (83) | 79π80π81σ-84π85π88π | 79π80π81π-84π86π88π | 67σ68σ76σ-84σ86σ89σ |
| 2 (91) | 86π88π89σ-92π93π97π | 86π88π89π-92π95π97π | 63σ73σ74σ-92σ94σ95σ |
| 3 (91) | 86π87π89σ-92π93π96π | 86π87π89π-92π94π95π | 73σ74σ84σ-92σ94σ95σ |
| 4 (95) | 91π92π93σ-96π97π99σ | 91π92π93π-96π98π99π | 74σ75σ88σ-96σ98σ100σ |
| 5 (89) | 85π86π88σ-90π92π93π | 85π86π88π-90π94π95π | 71σ73σ82σ-90σ94σ95σ |
| 6 (87) | 82π83π85σ-88π89π93π | 82π83π85π-88π90π92π | 68σ69σ80σ-88σ90σ93σ |
| 7 (91) | 86π87π89σ-92π93π97π | 86π87π89π-92π94π95π | 70σ72σ84σ-92σ94σ97σ |
| 8 (91) | 87π88π89σ-92π93π97π | 87π88π89π-92π96π97π | 73σ74σ84σ-92σ94σ96σ |
| 9 (91) | 87π88π89σ-92π93π97π | 87π88π89π-92π95π96π | 73σ74σ83σ-92σ95σ96σ |
| 10 (91) | 86π88π89σ-92π93π96π | 86π88π89π-92π94π95π | 72σ74σ83σ-92σ94σ95σ |
| 11 (99) | 94π96π97σ-100π101π105π | 94π96π97π-100π103π104π | 80σ82σ90σ-100σ103σ104σ |
| 12 (87) | 83π86σ87σ-88π89π93π | 83π86π87π-88π92π93π | 71σ72σ80σ-88σ92σ93σ |
| 13 (87) | 82π84π85σ-88π89π93π | 82π84π85π-88π90π91π | 71σ72σ80σ-88σ90σ91σ |
| 14 (83) | 79π80π82σ-84π85π86π | 79π80π82π-84π88π89π | 64σ66σ67σ-84σ87σ88σ |
| 15 (83) | 79π80π81σ-84π86π88π | 79π80π81π-84π88π89π | 67σ68σ77σ-84σ87σ88σ |
| 16 (96) | 91π92π93σ-97π99π102π | 91π92π93π-97π100π102π | 74σ76σ88σ-97σ100σ102σ |

**Table 8**: Local Molecular Orbitals of atoms 15, 21 and 23

| Molecule | Atom 15 (C) | Atom 21 (C) | Atom 23 (C) | Atom 24 (C) |
|---|---|---|---|---|
| 1 (83) | 75σ78σ83σ-86σ87σ88σ | 78π82π83π-86π87π88π | 78π82π83π-87π88π89π | 78σ82π83π-86π87π88π |
| 2 (91) | 78σ87σ91σ-94σ98σ100σ | 87π90π91π-94π95π96π | 87π90π91π-95π96π98π | 87π90π91σ-94π95π96π |
| 3 (91) | 82σ88σ91σ-94σ97σ101σ | 88π90π91π-94π95π97π | 88π90π91π-94π95π96π | 88π90π91π-94π95π97π |
| 4 (95) | 83σ86σ90σ-103σ104σ105σ | 90π94π95π-98π99π101π | 90π94π95π-99π100π101π | 90σ94π95π-98π99π100π |
| 5 (89) | 77σ83σ84σ-93σ96σ97σ | 84π87π89π-91π92π93π | 84π87π89π-91π93π102π | 84σ87π89π-91π92π93π |
| 6 (87) | 77σ79σ84σ-92σ95σ96σ | 79σ84π86π-90π91π92π | 84σ86π87π-91π92π93π | 84σ86π87π-90π91π92π |
| 7 (91) | 81σ82σ88σ-95σ96σ99σ | 88π90π91π-94π95π96π | 88π90π91π-94π95π96π | 88σ90π91σ-94π95π96π |
| 8 (91) | 78σ80σ86σ-94σ100σ101σ | 83σ86π90π-94π95π96π | 86π90π91π-94π95π96π | 86σ90π91σ-94π95π96π |
| 9 (91) | 82σ86σ91σ-94σ95σ99σ | 86π90π91π-94π96π99π | 86π90π91π-94π95π96π | 86π90π91π-94π95π96π |
| 10 (91) | 81σ82σ87σ-99σ101σ102σ | 87π90π91π-94π95π96π | 87π90π91π-94π95π96π | 87π90π91π-94π95π96π |
| 11 (99) | 88σ95σ99σ-102σ103σ108σ | 95σ98π99π-102π103π104π | 95π98π99π-102π103π104π | 95π98π99π-102π103π104π |
| 12 (87) | 79σ84σ87σ-90σ94σ96σ | 84π85π87σ-90π91π99σ | 85π86π87σ-90π91π105π | 84π85π87σ-90π91π100σ |
| 13 (87) | 76σ78σ83σ-95σ96σ98σ | 83π86π87π-90π91π92π | 83π86π87π-90π91π92π | 83σ86π87π-90π91π92π |
| 14 (83) | 75σ76σ83σ-87σ92σ93σ | 77π78π81σ-85π86π87π | 78π81σ83π-85π86π87π | 78π81σ83π-85π86π87π |
| 15 (83) | 75σ82σ83σ-88σ91σ92σ | 76π82σ83π-85π87π88π | 76π82σ83π-85π87π88π | 76π82σ83π-85π87π88π |
| 16 (96) | 90σ94σ96σ-98σ104σ106σ | 94π95π96π-98π101π105π | 90π94π95π-101π105π109π | 94π95π96π-101π105π113π |

Results for Group B

Figure 6 shows the common skeleton numbering of Group A that will be employed in the results and discussion.

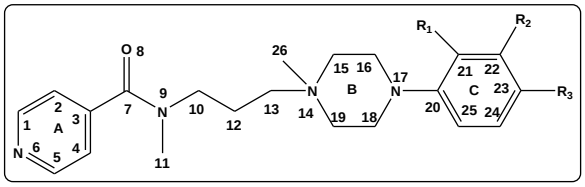


*Figure 6: Common skeleton numbering of group B*

Results for the 5-$HT_{1A}$ receptor binding affinity of Group B.

The best equation obtained is:

$$\log(IC_{50}) = -11.20 - 0.51S_{21}^{N}(LUMO)^{*} + 1.88\eta_{24} - 0.42S_{10}^{N}(LUMO+2)^{*} + \\ +4.90F_{13}(HOMO-2)^{*} \quad (3)$$

with n=16, R=0.97, $R^2$=0.94, adj-$R^2$=0.92, F(4,11)=41.63($p<0.000001$) and a standard error of estimate of0.23. No outliers were detected and no residuals fall outside the ±2σ limits. Here, $S_{21}^{N}$(LUMO)* is the nucleophilic superdelocalizability of the lowest empty MO localized on atom 21, $\eta_{24}$ is the local atomic hardness of atom 24, $S_{10}^{N}$(LUMO+2)* is the nucleophilic superdelocalizability of the third lowest empty MO localized on atom 10 and $F_{13}$(HOMO-2)* is the Fukui index of the third highest occupied MO localized on atom 13.Tables 9 and 10 show the beta coefficients, the results of the t-test for significance of coefficients and the matrix of squared correlation coefficients for the variables of Eq. 3. There are no significant internal correlations between independent variables (Table 10). Figure 7 displays the plot of observed *vs.* calculated log($IC_{50}$).

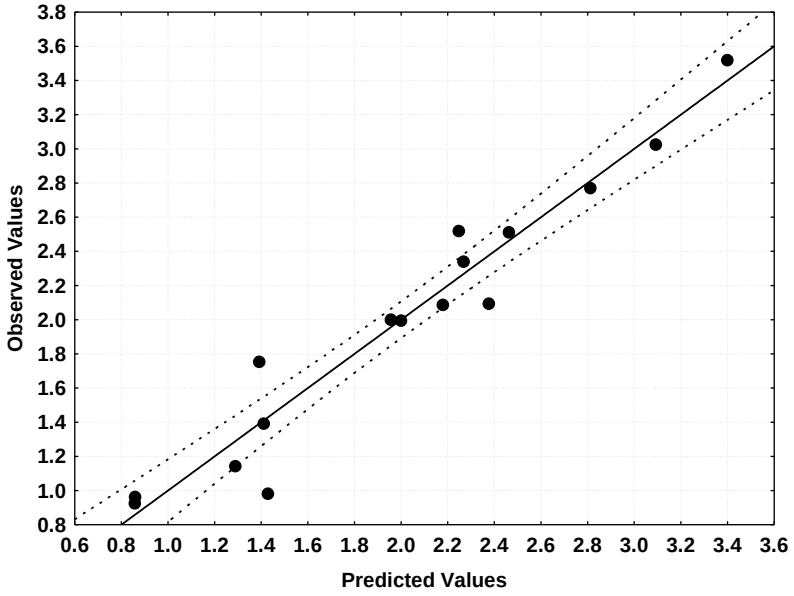


*Figure 7: Plot of predicted vs. observed log($IC_{50}$) values (Eq. 3). Dashed lines denote the 95% confidence interval*

**Table 9**: Beta coefficients and t-test for significance of coefficients in Eq. 3

| Variable | Beta | t(11) | p-level |
|---|---|---|---|
| $S_{21}^{N}$(LUMO)* | -1.17 | -11.17 | 0.000000 |
| $\eta_{24}$ | 0.68 | 8.40 | 0.000004 |
| $S_{10}^{N}$(LUMO+2)* | -0.42 | -5.20 | 0.0003 |
| $F_{13}$(HOMO-2)* | 0.34 | 3.50 | 0.005 |

**Table 10**: Matrix of squared correlation coefficients for the variables in Eq. 3

| | $S_{10}^{N}$(LUMO+2)* | $F_{13}$(HOMO-2)* | $S_{21}^{N}$(LUMO)* |
|---|---|---|---|
| $F_{13}$(HOMO-2)* | 0.07 | 1.00 | |
| $S_{21}^{N}$(LUMO)* | 0.12 | 0.41 | 1.00 |
| $\eta_{24}$ | 0.01 | 0.04 | 0.14 |

The associated statistical parameters of Eq. 3 indicate that this equation is statistically significant and that the variation of the numerical values of a group of four local atomic reactivity indices of atoms of the common skeleton explains about 92% of the variation of the receptor affinity. Figure 7, spanning about 2.6 orders of magnitude, shows that there is a good correlation of observed *versus* calculated values and that almost all points are inside the 95% confidence interval.

Results for the 5-$HT_{2A}$receptor binding affinity of Group B.
The best equation obtained was:

$$\log(IC_{50}) = 2.07 - 0.42S_{15}^{N}(LUMO+2)^{*} - 23.11F_{16}(HOMO-2)^{*} - 27.49F_{19}(LUMO+2)^{*} \quad (4)$$

with n=10, R=0.99, $R^2$=0.98, adj-$R^2$=0.97, F(3,6)=99.07($p<0.00002$) and a standard error of estimate of0.28. No outliers were detected and no residuals fall outside the $\pm 2\sigma$ limits. Here, $S_{15}^{N}$(LUMO+2)* is the nucleophilic superdelocalizability of the third lowest MO localized on atom 15, $F_{16}$(HOMO-2)* is the Fukui index of the third highest occupied MO localized on atom 16 and $F_{19}$(LUMO+2)* is the Fukui index of the third lowest empty MO localized on atom 19.Tables 11 and 12 show the beta coefficients, the results of the t-test for significance of coefficients and the matrix of squared correlation coefficients for the variables of Eq. 4. There are no significant internal correlations between independent variables (Table 12). Figure 8 displays the plot of observed *vs.* calculated $\log(IC_{50})$.

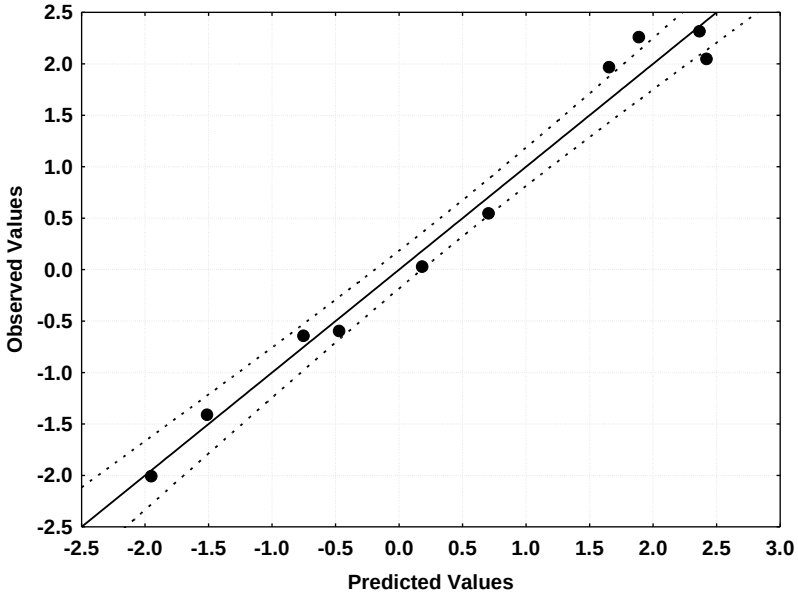


*Figure 8: Plot of predicted vs. observed log($IC_{50}$) values (Eq. 4). Dashed lines denote the 95% confidence interval.*

**Table 11**: Beta coefficients and t-test for significance of coefficients in Eq. 4

| Variable | Beta | t(6) | p-level |
|---|---|---|---|
| $S_{15}^{N}$(LUMO+2)* | -0.33 | -5.21 | 0.002 |
| $F_{16}$(HOMO-2)* | -0.39 | -6.29 | 0.0007 |
| $F_{19}$(LUMO+2)* | -0.93 | -15.49 | 0.000005 |

**Table 12**: Matrix of squared correlation coefficients for the variables in Eq. 4

| | $S_{15}^{N}$(LUMO+2)* | $F_{16}$(HOMO-2)* |
|---|---|---|
| $F_{16}$(HOMO-2)* | 0.13 | 1.00 |
| $F_{19}$(LUMO+2)* | 0.08 | 0.01 |

The associated statistical parameters of Eq. 4 indicate that this equation is statistically significant and that the variation of the numerical values of a group of three local atomic reactivity indices of atoms of the common skeleton explains about 97% of the variation of the receptor affinity. Figure 8, spanning about 4.5 orders of magnitude, shows that there is a good correlation of observed *versus* calculated values and that almost all points are inside the 95% confidence interval.

Local Molecular Orbitals

Table 13 shows the local molecular orbitals of atoms 10, 13 and 15. Table 14 shows the local molecular orbitals of atoms 16, 19, 21 and 24 (see Fig. 6). Nomenclature: Molecule (HOMO) / (HOMO-2)* (HOMO-1)* (HOMO)* - (LUMO)* (LUMO+1)* (LUMO+2)*.

**Table 13**: Local Molecular Orbitals of atoms 10, 13 and 15

| Molecule | Atom 10 (C) | Atom 13 (C) | Atom 15 (C) |
|---|---|---|---|
| 1 (87) | 80σ81σ82σ-93σ94σ95σ | 74σ75σ80σ-90σ91σ92σ | 74σ83σ87σ-90σ94σ95σ |
| 2 (95) | 88σ89σ90σ-102σ104σ105σ | 80σ83σ88σ-98σ101σ103σ | 82σ86σ93σ-98σ101σ103σ |
| 3 (95) | 87σ89σ90σ-101σ102σ103σ | 81σ82σ87σ-99σ101σ102σ | 80σ82σ93σ-99σ102σ103σ |
| 4 (99) | 92σ93σ94σ-105σ106σ107σ | 84σ85σ92σ-103σ105σ106σ | 86σ90σ98σ-103σ106σ107σ |
| 5 (93) | 86σ87σ88σ-94σ99σ101σ | 78σ79σ80σ-98σ99σ101σ | 80σ82σ93σ-98σ99σ102σ |
| 6 (91) | 84σ85σ86σ-97σ98σ99σ | 77σ78σ84σ-94σ95σ96σ | 83σ87σ91σ-94σ95σ98σ |
| 7 (95) | 88σ89σ90σ-101σ102σ103σ | 80σ81σ88σ-98σ101σ102σ | 84σ92σ95σ-98σ102σ103σ |
| 8 (95) | 87σ89σ90σ-101σ102σ104σ | 81σ82σ87σ-99σ100σ101σ | 82σ84σ91σ-98σ99σ100σ |
| 9 (95) | 87σ88σ90σ-101σ102σ103σ | 81σ82σ87σ-98σ99σ100σ | 82σ91σ95σ-98σ99σ100σ |
| 10 (95) | 87σ88σ89σ-101σ102σ103σ | 80σ81σ87σ-98σ99σ100σ | 84σ86σ91σ-98σ99σ100σ |
| 11 (103) | 94σ96σ97σ-109σ111σ112σ | 87σ88σ94σ-106σ108σ109σ | 88σ89σ99σ-107σ108σ110σ |
| 12 (91) | 84σ85σ86σ-97σ98σ100σ | 78σ79σ84σ-96σ97σ98σ | 78σ83σ91σ-96σ98σ99σ |
| 13 (91) | 84σ85σ86σ-97σ98σ99σ | 79σ80σ84σ-94σ95σ96σ | 80σ87σ91σ-94σ95σ96σ |
| 14 (87) | 79σ81σ82σ-93σ94σ96σ | 75σ76σ79σ-91σ92σ93σ | 74σ80σ87σ-91σ92σ94σ |
| 15 (87) | 81σ82σ83σ-93σ94σ95σ | 75σ76σ81σ-92σ93σ94σ | 78σ80σ87σ-91σ92σ94σ |
| 16 (100) | 92σ93σ94σ-106σ107σ110σ | 83σ85σ92σ-105σ106σ107σ | 86σ88σ98σ-105σ107σ108σ |

**Table 14**: Local Molecular Orbitals of atoms 16, 19, 21 and 24

| Molecule | Atom 16 (C) | Atom 19 (C) | Atom 21 (C) | Atom 24 (C) |
|---|---|---|---|---|
| 1 (87) | 78σ79σ83σ-90σ91σ95σ | 77σ78σ83σ-90σ91σ92σ | 83σ86π87π-90π91π92π | 83π86π87π-90π91π92π |
| 2 (95) | 82σ91σ93σ-97σ101σ103σ | 82σ86σ93σ-98σ101σ104σ | 91π93σ95π-97π100π101σ | 87π93σ95π-97π100π111σ |
| 3 (95) | 88σ93σ95σ-98σ100σ105σ | 80σ82σ93σ-99σ100σ102σ | 93σ94π95π-98π100π111σ | 93σ94π95π-98π100π108σ |
| 4 (99) | 88σ97σ98σ-102σ104σ107σ | 86σ90σ98σ-103σ104σ105σ | 97π98σ99π-102π103π104π | 91π98σ99π-102π103π104π |
| 5 (93) | 84σ90σ93σ-95σ96σ98σ | 80σ82σ93σ-98σ102σ103σ | 90π91π93σ-95π96π100σ | 84π85σ91π-95π96π106π |
| 6 (91) | 81σ83σ87σ- | 78σ81σ87σ- | 87σ90π91π- | 87σ90π91π- |

| | | | | |
|---|---|---|---|---|
| | 94σ99σ101σ | 94σ95σ98σ | 95π96π98π | 95π96π98π |
| 7 (95) | 85σ86σ92σ-<br>99σ103σ105σ | 85σ86σ92σ-<br>98σ99σ102σ | 92σ94π95π-<br>98π99π100π | 92σ94π95π-<br>98π99π100π |
| 8 (95) | 88σ91σ95σ-<br>98σ100σ104σ | 82σ91σ95σ-<br>99σ100σ101σ | 91σ94π95π-<br>98π99π101σ | 91σ94π95π-<br>98π99π102σ |
| 9 (95) | 85σ86σ91σ-<br>103σ106σ107σ | 84σ86σ91σ-<br>98σ99σ100σ | 91σ94π95π-<br>98π99π100π | 91π94π95π-<br>98π99π100π |
| 10 (95) | 86σ91σ95σ-<br>98σ100σ103σ | 79σ80σ91σ-<br>98σ99σ100σ | 91σ93π95π-<br>98π99π100π | 91π93π95π-<br>98π99π102π |
| 11 (103) | 90σ92σ99σ-<br>112σ114σ115σ | 89σ92σ99σ-<br>106σ107σ108σ | 99σ102π103π-<br>106π107π108π | 99π102π103π-<br>106π107π110σ |
| 12 (91) | 83σ88σ91σ-<br>93σ98σ99σ | 78σ83σ91σ-<br>96σ98σ100σ | 83σ89π91σ-<br>93π95π98σ | 83σ89π91σ-<br>93π95π109σ |
| 13 (91) | 80σ82σ87σ-<br>99σ101σ102σ | 80σ82σ87σ-<br>94σ95σ96σ | 87σ89π91π-<br>94π95π96π | 87π89π91π-<br>94π95π96π |
| 14 (87) | 77σ80σ87σ-<br>91σ94σ97σ | 75σ80σ87σ-<br>91σ92σ94σ | 83π84σ87π-<br>89π91π92π | 83π84σ87π-<br>89π91π92π |
| 15 (87) | 80σ86σ87σ-<br>92σ95σ97σ | 78σ80σ87σ-<br>91σ92σ94σ | 81σ86σ87π-<br>89π91π92π | 80σ86σ87π-<br>89π91π92π |
| 16 (100) | 88σ95σ98σ-<br>102σ108σ109σ | 86σ88σ98σ-<br>105σ106σ107σ | 98σ99π100π-<br>102π104π108π | 95π98σ99π-<br>104π107π108π |

**Discussion**

The discussion will be separated in two sections corresponding to each kind of receptor, allowing a better integration of results.

Discussion of the results of the 5-$HT_{1A}$receptor binding affinity of Groups A and B.

Discussion of the 5-$HT_{1A}$ receptor binding affinity of Group A.

For group ATable 5 shows that the importance of variables in Eq. 1 is$\varphi_4$>>$S_{12}^{E}$(HOMO-2)*>> $F_4$(LUMO)*> $S_{19}^{E}$. In the following discussions we shall employ the approximate variable-by-variable (VbV) method. By considering the sign associated to each variable in Eq. 1 together with the positive or negative value of the local atomic reactivity indices, a high receptor affinity is associated with small values of $\varphi_4$, large (negative) values of $S_{19}^{E}$, small (negative) values of $S_{12}^{E}$(HOMO-2)* and large values of $F_4$(LUMO)*.$\varphi_4$ is the orientational parameter of the $R_4$ substituent. A small value of the OP demands a small substituent, like H.Table 1 suggests that, for getting more information about the nature of an appropriate $R_4$ substituent, a methyl group will be apt. Another possibility is simply substituting the carbon atom 22 by a nitrogen atom. On the other hand we need to consider that the modification of $R_4$ must not alter in a significant way the electronic structure of the system.Atom 12 is a hydrogen atom attached to N9 (see Fig. 3). All local MOs are of σ nature (Table 7). In all molecules the local $(HOMO)_{12}^{*}$ is situated very far from the corresponding molecular HOMO (Table 7). Small (negative) values of $S_{12}^{E}$(HOMO-2)* are associated with high receptor affinity. Small values for this index are obtained by lowering the associated eigenvalue and/or by lowering the electron population of this MO. On this basis we suggest that the H atom is participating in an N-H…X hydrogen bond.Atom 4 is a carbon atom in ring A (Fig. 3). A high receptor affinity is associated with large values of $F_4$(LUMO)*. Table 7 shows that the local $(LUMO)_4^{*}$ has a π nature and that it coincides with the molecular LUMO. Note also that all $(HOMO)_4^{*}$ have a σ nature in all molecules Therefore, we suggest that atom 4 is interacting with an electron rich center, possible of the π-π kind.Atom 19 is a carbon atom in ring C (Fig. 3). A high receptor affinity is associated with large (negative) values of $S_{19}^{E}$, suggesting that this atom is acting as an electron donor.All the above suggestions are displayed in the partial 2D pharmacophore of Fig. 9.

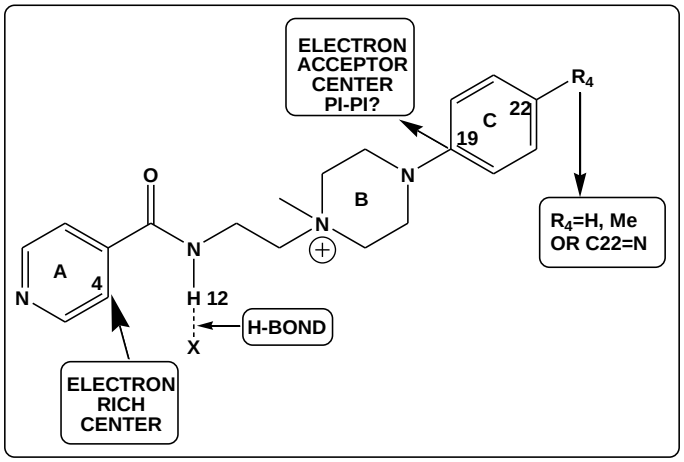


*Figure 9: Partial 2D pharmacophore for the 5-$HT_{1A}$ binding affinity of group A.*

Discussion of the 5-$HT_{1A}$ receptor binding affinity of Group B.

For group B Table 9 shows that the importance of variables in Eq. 3 is $S_{21}^{N}$(LUMO)*> $\eta_{24}$> $S_{10}^{N}$(LUMO+2)*> $F_{13}$(HOMO-2)*.By considering the sign associated to each variable in Eq. 3 together with the positive or negative value of the local atomic reactivity indices, we can see that a high receptor affinity is associated with a small value for $\eta_{24}$ and a small value for $F_{13}$(HOMO-2)*. If $S_{21}^{N}$(LUMO)* is positive, a high receptor affinity is associated with a high numerical value for this reactivity index. The same holds for the case of a positive value for $S_{10}^{N}$(LUMO+2)*. Atom 21 is a carbon in ring C (Fig. 6). Table 14 shows that $(LUMO)_{21}^{*}$ has a π nature in all molecules. A high receptor affinity is associated with high numerical values for $S_{21}^{N}$(LUMO)*. These values are obtained by lowering the energy of this MO, making it more reactive. Therefore, it is suggested that this atom is interacting with an electron-rich center (probably through a π-π interaction).Atom 24 is a carbon in ring C (Fig. 6). A high receptor affinity is associated with low numerical values for this local atomic hardness,$\eta_{24}$ (the HOMO*-LUMO* energy gap). It is almost always a positive number (it has a zero value in the case of metals and in some atoms of semimetals). If we interpret the local atomic hardness as the resistance of an atom to exchange electrons with the milieu, a small value indicates that, for a higher receptor affinity, atom 24 should be more reactive. Now, Table 14 shows that in almost all molecules the local HOMO* coincides with the molecular HOMO, while the local LUMO* corresponds to higher empty molecular MOs. Then, the only way to get a smaller HOMO*-LUMO* energy gap is by shifting downwards the LUMO* eigenvalue energy. This suggests that atom 24 is interacting with an electron-rich center. Atom 10 is a saturated carbon in the chain linking N9 with ring B (Fig. 6). All local MOs have σ nature (Table 13). If $S_{21}^{N}$(LUMO)* is positive, then a high affinity is associated with high numerical values for this index. These values are obtained by shifting downwards the MO eigenvalue; making the MO more reactive.

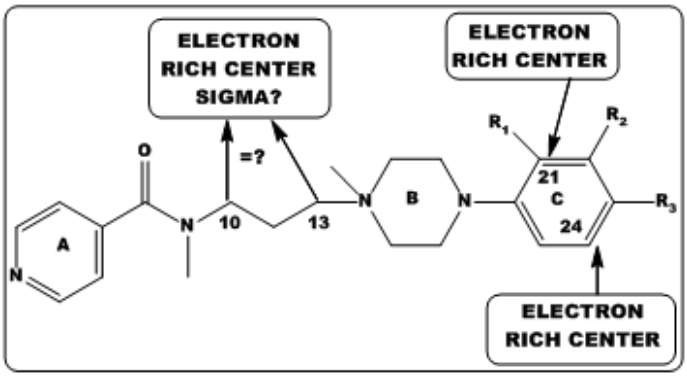


*Figure 10: Partial 2D pharmacophore for the 5-$HT_{1A}$ binding affinity of group B*

On this basis we suggest that atom 10 is interacting with an electron-rich center. Atom 13 is a saturated carbon in the chain linking N9 with ring B (Fig. 6). All local MOs have σ nature (Table 13). As $F_{13}$(HOMO-2)* is always positive, a high affinity is associated with a low electron population on this local MO*. We may observe also in Table 14 that the three highest occupied local MOs of atom 13 are far below from the molecule's HOMO, suggesting that this atom cannot act as an electron donor. Therefore, we suggest that atom 13 is interacting with an electron-rich center. All the above suggestions are displayed in the partial 2D pharmacophore of Fig. 10.

Discussion of the results of the 5-$HT_{2A}$ receptor binding affinity of Groups A and B.
Discussion of the 5-$HT_{2A}$ receptor binding affinity of Group A.
For group ATable 5 shows that the importance of variables in Eq. 2 is$S_8^E$(HOMO-1)*> $F_{15}$(HOMO-2)*> $S_{23}^N$(LUMO+2)*> $\mu_{10}$> $F_{21}$(HOMO-1)*.Analyzing the sign associated with each variable in Eq. 2 together with the positive or negative value of the local atomic reactivity indices, we can see that a high receptor affinity is associated with low numerical values for $S_8^E$(HOMO-1)* (that is always a negative number), high numerical values for $F_{15}$(HOMO-2)* (that is always a positive number), small numerical values for $\mu_{10}$ (that is always a negative number) and small numerical values for $F_{21}$(HOMO-1)*. If $S_{23}^N$(LUMO+2)* is a positive number, then a high affinity is associated with small numerical values for this index. Atom 8 is a carbonyl oxygen atom in the chain linking rings A and B (Fig. 3). Table 7 shows that the three lowest empty and the three highest occupied MOs have π nature and that only the local LUMO* coincides with the molecular LUMO. Small negative values for $S_8^E$(HOMO-1)* are obtained by lowering the $(HOMO\text{-}1)_8^*$ energy, making this MO less reactive. This allows us to suggest that atom 8 is interacting with the receptor as an electron acceptor. Atom 15 is a saturated carbon atom in ring B (Fig. 3). Table 7 shows that all local MOs have σ nature. High numerical values for $F_{15}$(HOMO-2)* are obtained by increasing the electron population on this MO. This suggests that atom 15 is interacting with an electron deficient center. Atom 10 is a saturated carbon atom in the chain linking rings A and B (Fig. 3). Table 7 shows that all local MOs have σ nature. $\mu_{10}$ is the local atomic electronic chemical potential of atom 10. A high affinity is associated with small numerical negative values for $\mu_{10}$. For reasons exposed in another paper [37], the best way to get these values is by shifting upwards the energy of the local LUMO*; making this MO less reactive. Therefore, we suggest that atom 10 is interacting with an electron-deficient center. This coincides with the standard interpretation stating that a small negative value of this index implies a good electron donor. Atom 23 is a carbon atom in ring C (Fig. 3). Table 8shows that all molecules but one the local HOMO*s of this atom have π nature. If $S_{23}^N$(LUMO+2)* is positive, a high affinity is related to small numerical values for this index. These values are obtained by shifting upwards the energy of this local MO; making it less reactive. This suggests that this atom is interacting with an electron-deficient center. Atom 21 is a carbon atom in ring C (Fig. 3). Table 8 shows that all molecules but one the local (HOMO-1)*s of this atom have π nature. The analysis of this index suggests that this atom is interacting with an electron-rich center. All the above suggestions are displayed in the partial 2D pharmacophore of Fig. 11.

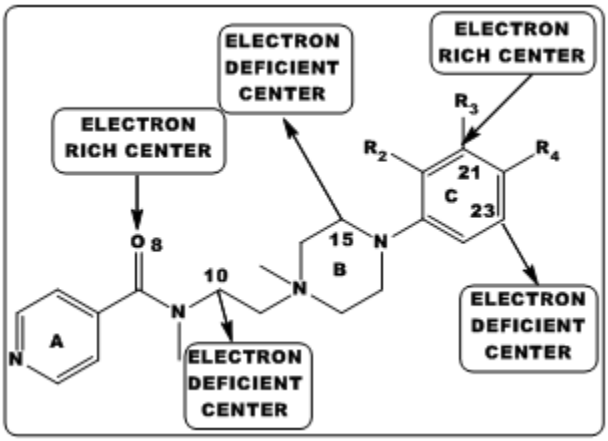


*Figure 11: Partial 2D pharmacophore for the 5-$HT_{2A}$ binding affinity of group A*

Discussion of the 5-$HT_{2A}$ receptor binding affinity of Group B.

For group BTable 11 shows that the importance of variables in Eq. 4 is $F_{19}$(LUMO+2)*>> $F_{16}$(HOMO-2)*> $S_{15}^{N}$(LUMO+2)*. Analyzing the sign associated with each variable in Eq. 4 and the positive or negative value of the local atomic reactivity indices, we can see that a high 5-$HT_{2A}$ receptor affinity is associated with small numerical values for $F_{16}$(HOMO-2)* and $F_{19}$(LUMO+2)*. If the numerical value of $S_{15}^{N}$(LUMO+2)* is positive, then a high affinity is associated with high numerical values for this index. Atom 15 is a carbon in ring B (Fig. 6). All local MOs have σ nature (Table 13). High positive numerical values for this index are obtained by shifting downwards the value corresponding eigenvalue; making this MO more reactive. Therefore, it is suggested that atom 15 is interacting with an electron-rich center. Atom 16 is a carbon in ring B (Fig. 6). All local MOs have σ nature (Table 14).Small numerical values for $F_{16}$(HOMO-2)* are obtained by incrementing the electron population of $(HOMO-2)_{16}$*. Accordingly to this, atom 16 should be interacting with an electron-deficient center. Atom 19 is a carbon in ring B (Fig. 6). All local MOs have σ nature (Table 14).Small numerical values for $F_{19}$(LUMO+2)* are obtained by diminishing the electron population of $(LUMO+2)_{19}$*. Therefore, it is suggested that atom 19 is interacting with an electron-deficient center. All the above suggestions are displayed in the partial 2D pharmacophore of Fig. 12.

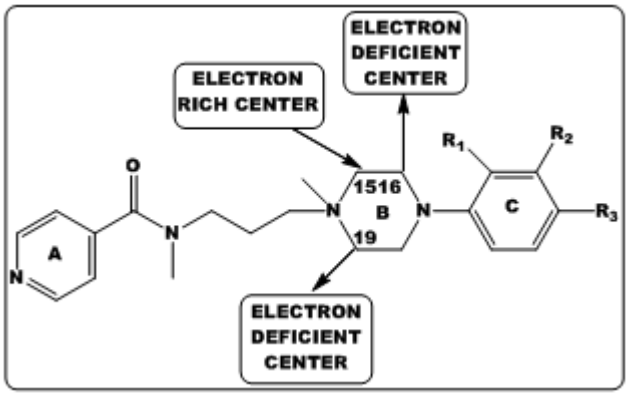


*Figure 12: Partial 2D pharmacophore for the 5-$HT_{2A}$ binding affinity of group B*

Integration of pharmacophores.

For both series of molecules we may integrate the partial 2D pharmacophores for the binding to each receptor to have an approximate view of what could be happening. For the integration, we have assumed that rings A and C (the aromatic ones) of both series of molecules bind to the same sites of the receptor.

2D pharmacophore integration for 5-$HT_{1A}$ binding.

Figure 13 shows the integrated pharmacophore.

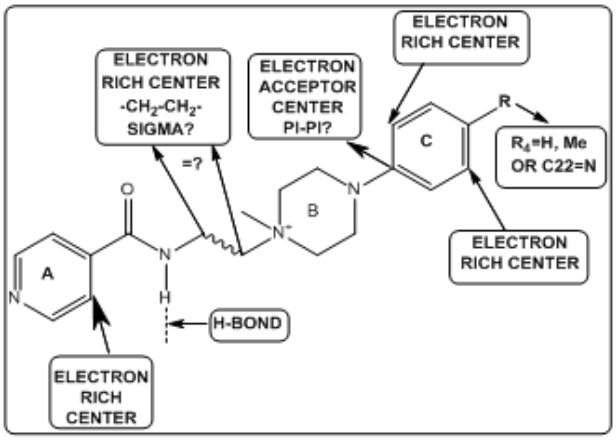


*Figure 13: Partial 2D integrated pharmacophore for 5-$HT_{1A}$ binding of groups A and B.*

The integrated partial pharmacophore allow suggesting that rings A and C are interacting with sites having π electrons (aromatic rings, carboxylate moieties, etc.). In a recent analysis of the interaction of 2,5-dimethoxyphenethylamines and their N-2-methoxybenzyl-substituted analogs with 5-$HT_{1A}$ serotonin receptors[1] it was suggested that the methanediyl groups of the ethylamine side chain seemed to interact with a site or sites having sigma electrons. If the integration presented here is correct, then we are again in presence of a three dimensional receptor site having occupied σ MOs (in ancient chemistry these sites were called sometimes "hydrophobic pockets"). The appearance in ring C of three carbon atoms strongly suggests that this ring is involved in π-π aromatic interactions with the receptor.

2D pharmacophore integration for 5-$HT_{2A}$ binding.

Figure 14 shows the integrated pharmacophore.

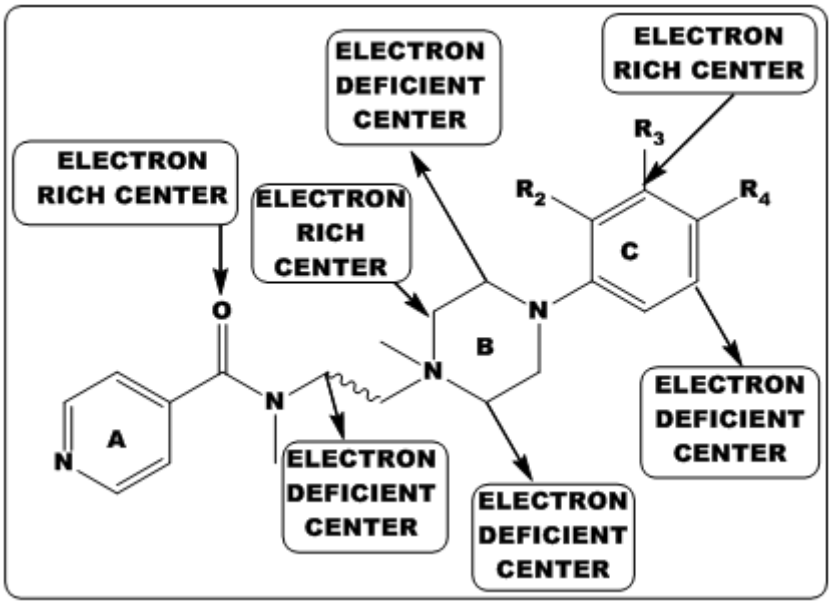


*Figure 14: Partial 2D integrated pharmacophore for 5-$HT_{2A}$ binding of groups A and B.*

The analysis of Fig. 14 again suggests the presence of a site rich in sigma electrons but now in the 5-$HT_{2A}$ receptor. Again ring C seems to interact with a site through π-π interactions. This similitude between the integrated pharmacophores suggests two possibilities. The first one states that this is only a mere coincidence. The second one states that both receptors have a similar binding volume conserved during evolution.

**References**

1. J. S. Gómez-Jeria, C. Moreno-Rojas, Chemistry Research Journal, 2017, 2, 27.
2. J. S. Gómez-Jeria, M. B. Becerra-Ruiz, International Journal of Advances in Pharmacy, Biology and Chemistry, 2017, 6, 72.
3. S. Aznar, M. E.-S. Hervig, Neuroscience & Biobehavioral Reviews, 2016, 64, 63.
4. S. Köhler, K. Cierpinsky, G. Kronenberg, M. Adli, Journal of Psychopharmacology, 2016, 30, 13.
5. M. Oostland, J. A. van Hooft, "Serotonin in the Cerebellum," in *Essentials of Cerebellum and Cerebellar Disorders: A Primer For Graduate Students*, D. L. Gruol, N. Koibuchi, M. Manto, M. Molinari, J. D. Schmahmann, and Y. Shen Eds., pp. 243, Springer International Publishing, Cham, 2016.
6. J. M. Palacios, Brain Research, 2016, 1645, 46.
7. R. Kraehenmann, D. Pokorny, L. Vollenweider, K. H. Preller, T. Pokorny, E. Seifritz, F. X. Vollenweider, Psychopharmacology, 2017, 234, 2031.
8. J. F. López-Giménez, J. González-Maeso, "Hallucinogens and Serotonin 5-HT2A Receptor-Mediated Signaling Pathways," in *Curr Top Behav Neurosci.*, pp. 1, Springer, Berlin, Heidelberg, 2017.

9. D. Wacker, S. Wang, J. D. McCorvy, R. M. Betz, A. J. Venkatakrishnan, A. Levit, K. Lansu, Z. L. Schools, T. Che, D. E. Nichols, B. K. Shoichet, R. O. Dror, B. L. Roth, Cell, 2017, 168, 377.
10. J. S. Gómez-Jeria, A. Robles-Navarro, Res. J. Pharmac. Biol. Chem. Sci., 2015, 6, 1358.
11. J. S. Gómez-Jeria, A. Robles-Navarro, J. Comput. Methods Drug Des., 2015, 5, 45.
12. J. S. Gómez-Jeria, A. Robles-Navarro, Der Pharma Chem., 2015, 7, 243.
13. P. Richter, A. Morales, J. S. Gomez-Jeria, D. Morales-Lagos, Analyst, 1988, 113, 859.
14. J. S. Gómez-Jeria, B. K. Cassels, J. C. Saavedra-Aguilar, Eur. J. Med. Chem., 1987, 22, 433.
15. J. S. Gómez-Jeria, D. Morales-Lagos, B. K. Cassels, J. C. Saavedra-Aguilar, Quant. Struct.-Relat., 1986, 5, 153.
16. J. S. Gómez-Jeria, B. K. Cassels, R. E. Clavijo, V. Vargas, R. Quintana, J. C. Saavedra-Aguilar, Microgram (DEA), 1986, 19, 153.
17. J. S. Gómez-Jeria, D. Morales-Lagos, J. I. Rodriguez-Gatica, J. C. Saavedra-Aguilar, Int. J. Quant. Chem., 1985, 28, 421.
18. J. S. Gómez-Jeria, D. R. Morales-Lagos, J. Pharm. Sci., 1984, 73, 1725.
19. J. S. Gómez-Jeria, D. Morales-Lagos, "The mode of binding of phenylalkylamines to the Serotonergic Receptor," in *QSAR in design of Bioactive Drugs*, M. Kuchar Ed., pp. 145, Prous, J.R., Barcelona, Spain, 1984.
20. J. S. Gómez-Jeria, Acta sud Amer. Quím., 1984, 4, 1.
21. F. Fiorino, A. Ciano, E. Magli, B. Severino, A. Corvino, E. Perissutti, F. Frecentese, P. Di Vaio, A. A. Izzo, R. Capasso, P. Massarelli, C. Nencini, I. Rossi, E. Kędzierska, J. Orzelska-Gòrka, A. Bielenica, V. Santagada, G. Caliendo, European Journal of Medicinal Chemistry, 2016, 110, 133.
22. The results presented here are obtained from what is now a routinary procedure. For this reason, we built a general model for the paper's structure. This model contains *standard* phrases for the presentation of the methods, calculations and results because they do not need to be rewritten repeatedly.
23. J. S. Gómez-Jeria, J. Comput. Methods Drug Des., 2017, 7, 17.
24. J. S. Gómez-Jeria, Canad. Chem. Trans., 2013, 1, 25.
25. J. S. Gómez-Jeria, *Elements of Molecular Electronic Pharmacology (in Spanish)*, Ediciones Sokar, Santiago de Chile, 2013.
26. J. S. Gómez-Jeria, M. Ojeda-Vergara, J. Chil. Chem. Soc., 2003, 48, 119.
27. J. S. Gómez-Jeria, "Modeling the Drug-Receptor Interaction in Quantum Pharmacology," in *Molecules in Physics, Chemistry, and Biology*, J. Maruani Ed., vol. 4, pp. 215, Springer Netherlands, 1989.
28. J. S. Gómez-Jeria, Int. J. Quant. Chem., 1983, 23, 1969.
29. J. S. Gómez-Jeria, M. Flores-Catalán, Canad. Chem. Trans., 2013, 1, 215.
30. C. Barahona-Urbina, S. Nuñez-Gonzalez, J. S. Gómez-Jeria, J. Chil. Chem. Soc., 2012, 57, 1497.
31. A. Robles-Navarro, J. S. Gómez-Jeria, Der Pharma Chem., 2016, 8, 417.
32. G. A. Kpotin, G. S. Atohoun, U. A. Kuevi, A. Houngue-Kpota, J.-B. Mensah, J. S. Gómez-Jeria, J. Chem. Pharmac. Res., 2016, 8, 1019.
33. G. Kpotin, S. Y. G. Atohoun, U. A. Kuevi, A. Kpota-Hounguè, J.-B. Mensah, J. S. Gómez-Jeria, Der Pharm. Lett., 2016, 8, 215.
34. J. S. Gómez-Jeria, R. Salazar, Der Pharma Chem., 2016, 8, 1.
35. J. S. Gómez-Jeria, Í. Orellana, Der Pharma Chem., 2016, 8, 476.
36. J. S. Gómez-Jeria, C. Moreno-Rojas, Der Pharma Chem., 2016, 8, 475.
37. J. S. Gómez-Jeria, M. Matus-Perez, Der Pharma Chem., 2016, 8, 1.
38. J. S. Gómez-Jeria, P. Latorre-Castro, Der Pharma Chem., 2016, 8, 84.
39. J. S. Gómez-Jeria, G. A. Kpotin, Der Pharma Chem., 2016, 8, 213.
40. J. S. Gómez-Jeria, V. Gazzano, Der Pharma Chem., 2016, 8, 21.
41. J. S. Gómez-Jeria, R. Cornejo-Martínez, Der Pharma Chem., 2016, 8, 329.

42. J. S. Gómez-Jeria, P. Castro-Latorre, G. Kpotin, Der Pharma Chem., 2016, 8, 234.
43. J. S. Gómez-Jeria, H. R. Bravo, Der Pharma Chem., 2016, 8, 25.
44. J. S. Gómez-Jeria, S. Abarca-Martínez, Der Pharma Chem., 2016, 8, 507.
45. H. R. Bravo, B. E. Weiss-López, J. Valdebenito-Gamboa, J. S. Gómez-Jeria, Res. J. Pharmac. Biol. Chem. Sci., 2016, 7, 792.
46. M. J. Frisch, G. W. Trucks, H. B. Schlegel, G. E. Scuseria, M. A. Robb, J. R. Cheeseman, J. Montgomery, J.A., T. Vreven, K. N. Kudin, J. C. Burant, J. M. Millam, S. S. Iyengar, J. Tomasi, V. Barone, B. Mennucci, M. Cossi, G. Scalmani, N. Rega, G03 Rev. E.01, Gaussian, Pittsburgh, PA, USA, 2007.
47. J. S. Gómez-Jeria, D-Cent-QSAR: A program to generate Local Atomic Reactivity Indices from Gaussian 03 log files. v. 1.0, Santiago, Chile, 2014.
48. J. S. Gómez-Jeria, J. Chil. Chem. Soc., 2009, 54, 482.
49. J. S. Gómez-Jeria, STERIC: A program for calculating the Orientational Parameters of the substituents. Santiago, Chile, 2015.
50. J. S. Gómez-Jeria, Res. J. Pharmac. Biol. Chem. Sci., 2016, 7, 2258.
51. J. S. Gómez-Jeria, Res. J. Pharmac. Biol. Chem. Sci., 2016, 7, 288.
52. Statsoft, Statistica v. 8.0, 2300 East 14 th St. Tulsa, OK 74104, USA, 1984-2007.